Supporting Information

4D Imaging of ZnO-Coated Nanoporous Al_2O_3 Aerogels by Chemically-Sensitive Ptychographic Tomography: Implications for Designer Catalysts

Hao Yuan[1], Hui Yuan[2], Travis Casagrande[2], David Shapiro[3], Young-Sang Yu[3], Bjoern Enders,[4,5] Jonathan R. I. Lee[6], Anthony van Buuren[6], Monika M. Biener[6], Stuart A. Gammon[6], Theodore F. Baumann[6] and Adam P. Hitchcock[1*]

[1] *Dept. Chemistry & Chemical Biology, McMaster University, Hamilton, ON, L8S 4M1 Canada*

[2] *Canadian Centre for Electron Microscopy, McMaster University, Hamilton, ON, L8S 4M1 Canada*

[3] *Advanced Light Source, Lawrence Berkeley National Lab, Berkeley, CA 94720, USA*

[4] *National Energy Research Scientific Computing Center, Lawrence Berkeley National Lab, Berkeley, CA 94720, USA*

[5] *Dept of Physics, University of California Berkeley, Berkeley, CA 94720, USA*

[6] *Lawrence Livermore National Laboratory, Livermore, CA 94550 USA.*

Applied NanoMaterials last changed: 24 Dec 2020 * Corresponding author: aph@mcmaster.ca

SI-a. Effect of iteration number on the ptychographic reconstruction

Figure S1 shows how the ptychographic reconstruction using the relaxed averaged alternating reflection reconstruction (RAAR) algorithm implemented in the SHARP software (version 9.0.7) converges as a function of number of iterations. The reconstruction converges by 500 iterations. After 500 iterations the image and image quality does not change with further iterations.

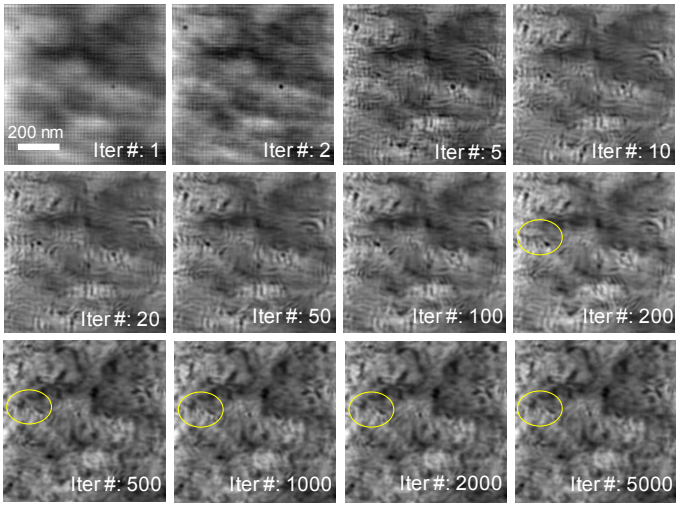

Figure S1. Dependence of the ptychographic reconstructed amplitude image of the **Xe FIB#2, sample F** at 1568 eV, on the number of iterations using the RAAR algorithm by SHARP software. The area in the yellow circle converges at 500 iterations.

Table S1 ZnO ALD coated Al_2O_3 aerogel samples: STXM and ptychography measurement details

CODE	# ALD cycles	Sample	Run	STXM	STXM dose (GGy) (±30%)	Ptychography	ptycho dose (GGy) (±30%)	Angles
A	25	cast from water suspension #1	Nov 16, ALS 5.3.2.1	Zn L stacks[(a)], maps	1.4	Zn L PST[(b)]	1	-65° to 65°, 14 angles
B	25	cast from water suspension #2	May 17, CLS aSTXM	Zn L, Al K[(c)], stacks, tomography	1.6	none	-	0° to 180°, 19 angles
C	6	cast from water suspension #3	May 17, ALS 11.0.2	Zn L, Al K, O K stacks, maps	2.2	none	-	
D	6	Ga FIB #1, prism, 20×20×30 um^3	May 17, CLS aSTXM	Zn L, Al K, stacks, tomography	1.2	none	-	0° to 180°, 19 angles
E	6	Xe plasma FIB #1, prism, 5×5×10 um^3	Oct 18, ALS COSMIC	Zn L stack, maps	1.0	Zn L PST[(a)]	6	-65° to 65°, 11 angles
F	6	Xe plasma FIB #2, cylinder, 3.5×3.5×10 um^3	Mar 19, ALS COSMIC	Zn L, Al K, stacks, map	0.4	Zn L, Al K PST[(b)]	9	-65° to 65°, 14 angles
F'	6	Xe plasma FIB #2, cylinder, 3.5×3.5×10 um^3	Jul 19, CLS aSTXM	Zn L, Al K, stacks, map	2.6	none	-	
G	6	Ga FIB #2, cylinder, 3.5×3.5×10 um^3	Jul 19, CLS aSTXM	Zn L, Al K, stacks, map	0.5	none	-	
H	12	Xe plasma FIB #3, cylinder, 3.5×3.5×10 um^3	Oct 19, ALS COSMIC	Zn L, Al K, stacks, map tomography	1.5	Zn L, Al K PST[(b)]	10	-80° to 80°, 17 angles

(a) Zn L-edge spectral stack scan: 1007-1018 (0.6 eV); 1018-1028 (0.3 eV); 1028-1060 (0.6 eV); 1060 –1085 (1.0 eV); 1085-11 25 (2.0 eV)
(b) PST - Ptychographic spectro-tomography (below and on peak or above edge)
(c) Al K-edge spectral stack scan: 1545-1552 (0.9 eV); 1552 – 1570 (0.4 eV); 1570 – 1600 (1.2 eV); 1600 – 1655 (3.0 eV)

SI-b. STXM Spectroscopy

Figure S2a presents the Zn L_{23} spectrum of pure ZnO which was isolated from the spectrum of the aerogel sample by subtracting a scaled version of the elemental response spectrum (OD1) of Al_2O_3 from the Zn L_{23} spectrum of **sample D**. **Figure S2b** presents the Al K spectrum of pure Al_2O_3 which was obtained by subtracting a scaled version of the elemental response spectrum (OD1) of ZnO from the Al K-edge spectrum of **sample D**.

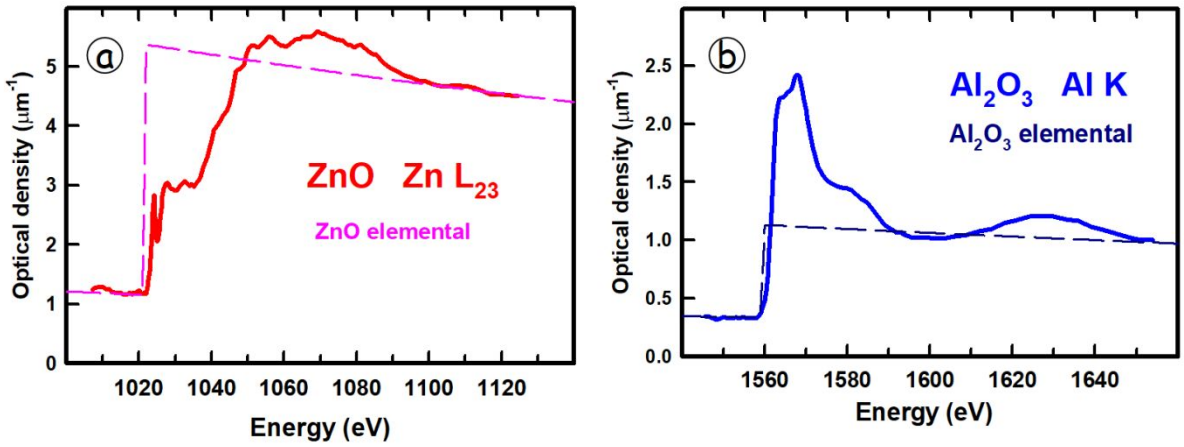

Figure S2 (a) ZnO L_{23} spectrum isolated from the spectrum of the 6-cycle ZnO/Al_2O_3 **sample D**, by subtracting a scaled version of the elemental response spectrum (OD1) of Al_2O_3 from the Zn L region. (b) Al K spectrum of Al_2O_3 obtained by subtracting a scaled version of the elemental response spectrum (OD1) of ZnO from the Al K spectrum of **sample D**. The dashed lines are the elemental response of ZnO (d = 5.61 g.cm^{-3}) and Al_2O_3 (d = 3.95 g.cm^{-3}) used to set absolute OD response per nm thickness. (COSMIC – Oct 2019)

SI-c Al K-edge compared to literature results for various Al compounds

Figure S3 compares the Al K-edge spectrum of 6 cycle (**Sample F**) and 25 cycle (**Sample D**) ZnO coated Al_2O_3 aerogel, compared with the Al K-edge spectra of α- Al_2O_3 (corundum) in which all the Al are in AlO_6 environments; mordenite, an aluminosilicate zeolite in which all the Al is in AlO_4 environments, and θ-Al_2O_3 in which there is a 50:50 ratio of AlO_4 and AlO_6 environments. These spectra were digitized from the literature [24-26]. The much broader Al K-edge spectrum of the aerogel indicates there is a large variety in local environments of the Al in the aerogel.

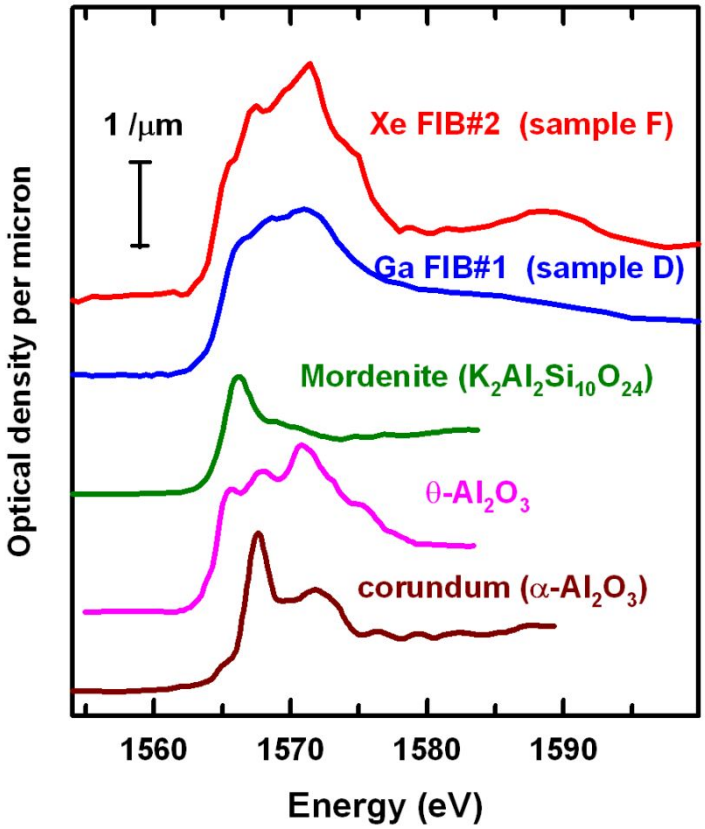

Figure S3. Al K-edge spectrum of Al_2O_3 of 6 cycle (**Sample F**) and 25 cycle (**Sample D**), compared with the Al K-edge spectra of corundum (α-Al_2O_3), θ-Al_2O_3 and mordenite, digitized from the literature [24-26].

SI-d Quantitative compositional analysis from STXM

Table S2 summarizes quantitative compositional information for all 6 samples studied. It reports the thickness of ZnO and Al_2O_3 (as if they were at standard bulk densities) derived from the quantitative STXM OD data and the OD1 reference spectra. The reported values are the average over the volumes imaged by STXM stacks.

Table S2 Average compositional information (nm thickness at normal density) and ratio derived from Zn L and Al K-edge spectroscopy

Sample →	A	H	D	E	F, F'	G
# ALD cycles	25	12	6	6	6	6
ZnO (nm) [(a)]	95	104	211	105	56	45
Al_2O_3 (nm) [(b)]	87	180	500	268	152	130
ZnO / Al_2O_3 [(c)]	1.09	0.58	0.42	0.39	0.37	0.35

(a) The ZnO thickness is determined from the OD from 1010-1160 eV over an area of uniform composition in the Zn L-edge STXM stack measured for the indicated ZnO/Al_2O_3 aerogel species, ratio-ed to the integrated OD1 of ZnO over the same energy range. Estimated uncertainty is 10% of the value. [OD1 is the optical density of a chemical species with 1 nm thickness at the normal density of that species].

(b) The Al_2O_3 thickness is the determined from OD from 1540-1660 eV over the same area of uniform composition in the Al K-edge STXM stack measured for the indicated ZnO/Al_2O_3 aerogel species, ratio-ed to the integrated OD1 of Al_2O_3 over the same energy range. Estimated uncertainty is 10% of the value.

(c) The compositional ratio is the ratio of the ZnO thickness (at normal density) to the Al_2O_3 thickness (at normal density) for each ZnO/Al_2O_3 aerogel species.

SI-e Sample modification by focussed ion beam milling (FIB)

In the previous report [7] significant depletion of ZnO was observed at the edges of the 20×20×30 μm cube prepared by Ga FIB. In the 6-cycle and 12-cycle samples, depletion of ZnO at the edges was also observed, despite efforts to reduce ion beam related sample damage. In the Xe FIB#3 (**sample H**) the depletion of ZnO extended a few hundred nm into the pillar (see **Fig. S4a, S4c**) probably caused by modification of the sample by the Xe plasma beam. We expect this occurs because ZnO is preferentially sputtered relative to Al_2O_3 by either ion beam, and the Xe plasma beam penetrates a significant depth into the highly porous aerogel. The ZnO depletion at the surface of the Ga FIB#2 pillar (**sample G**) was greater and extended over a micron into the edges of the sample (see **Fig. S4b, 4d**). The composition profiles were generated by averaging horizontal line profiles over the region in the yellow box (**Fig. S4c**) and over the whole portion displayed ((**Fig. S4d**).

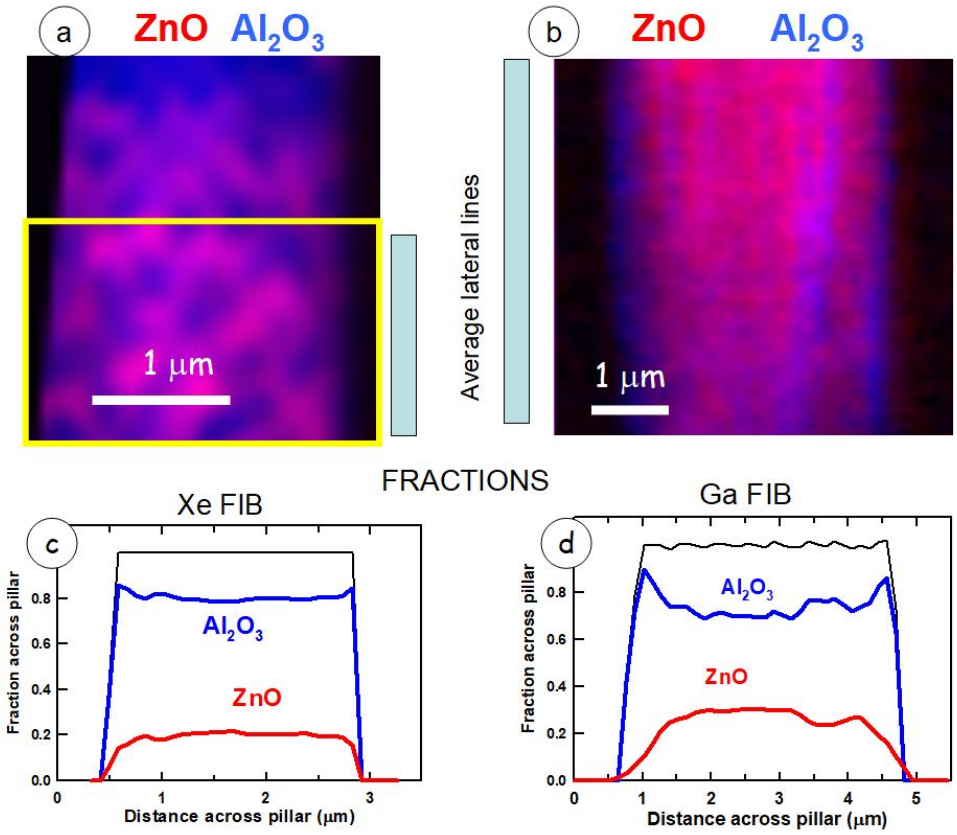

Figure S4. (a) Color coded composite map (ZnO in red, Al_2O_3 in blue) from STXM of **sample H** (Xe FIB#3). Only the region at the bottom (indicated by the yellow box) was included in generating the compositional profiles. (b) Rescaled, color-coded composite of the ptychography projections of Al_2O_3 (OD_{1568}–OD_{1550}, red) and ZnO (OD_{1050}–OD_{1015}, blue) of **sample G** (Ga FIB#2). The whole region was included in generating the compositional profiles. (c) Fractional compositional profiles across the pillar of **sample H**. (d) Fractional compositional profiles across the pillar of **sample G**.

SI-f Results from sample H

Figure S5 presents results from the 12-cycle, Xe FIB#3 **sample H**. **Figure S5a** is an SEM image recorded at the end of the sample preparation. **Figure S5b** is a Al-edge STXM image, indicating the distortion of the sample due to an unfortunate collision while introducing the sample into the COSMIC tomography end station. Despite that, it was possible to measure ptychographic maps and tomography data sets, and do a sufficiently high quality ptychography reconstruction, alignment and tomographic reconstruction to obtain meaningful results.

The reconstruction used a pixel size of 4.8 nm and voxel size of 4.8^3 nm^3, respectively. **Figure S5c** is a color-coded composite of the 2D ZnO and Al_2O_3 maps derived from 4-energy ptychography imaging. **Figure S5d** is an expansion of the region in the green box of **Fig. S5c**. **Figure S5e** is a surface rendering of the 3D reconstruction of spectro-ptycho-tomography recorded in the yellow box region indicated in **Fig. S5b**. In color images, ZnO is red and Al_2O_3 is blue.

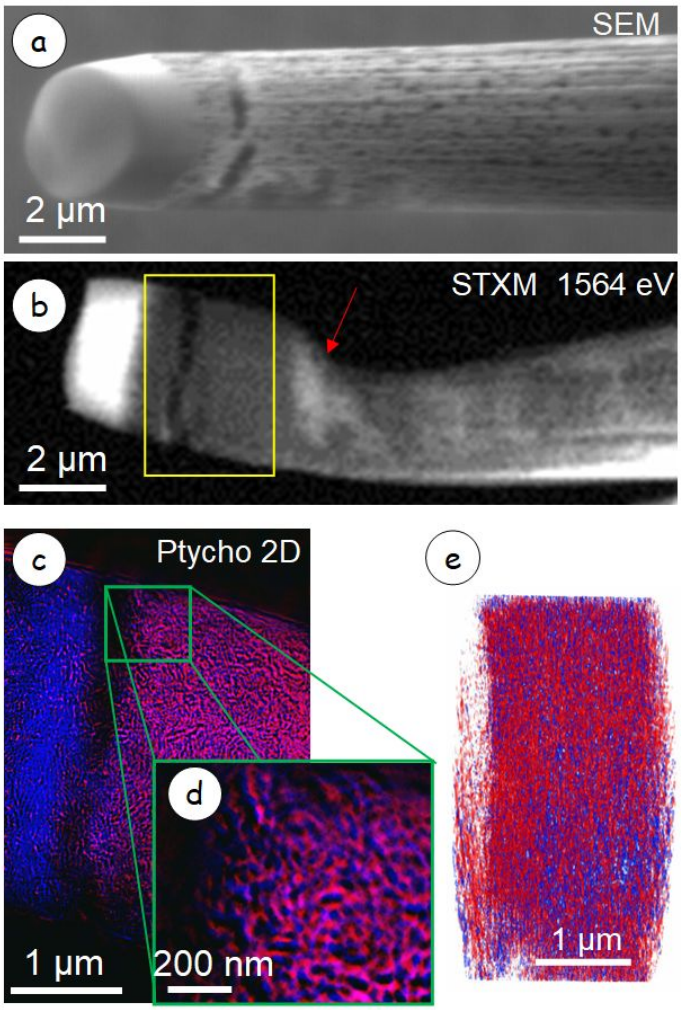

Figure S5 (a) SEM image of Xe FIB#3, **sample H**. (b) STXM OD image at 1568 eV. The yellow box is the region where spectro-ptycho-tomography was measured. The red arrow indicates the collision region caused by the sample loading accident. (c) color coded composite of the 2D ZnO and Al_2O_3 maps derived from 4-energy ptychography imaging. (d) expansion in green box area of (c). (e) 3D surface rendering of the 3D reconstruction of spectro-ptycho-tomography, Otsu thresholds of 4.72×10^{-4} (Al_2O_3) and 5.41×10^{-4} (ZnO). In color images, ZnO is red and Al_2O_3 is blue. (COSMIC – Oct 2019)

SI-g Comparing 2D spatial resolution of ptychography on BL 5.3.2.1 and COSMIC

Figure S6 compares Fourier Ring Correlation evaluations of the 2D spatial resolution achieved in earlier spectro-ptycho results on the same type of sample, but water cast, using NanoSurveyor-1 on ALS bend magnet BL 5.3.2.1 (25-cycle, **sample A** [7]) (**Fig. S6 a,b**) with that achieved on 6-cycle **sample E** (Xe FIB #1) using the COSMIC beamline in Oct 2018 (**Fig. S6 c,d**). The 2D spatial resolution was improved from ~15 nm, to ~6 nm.

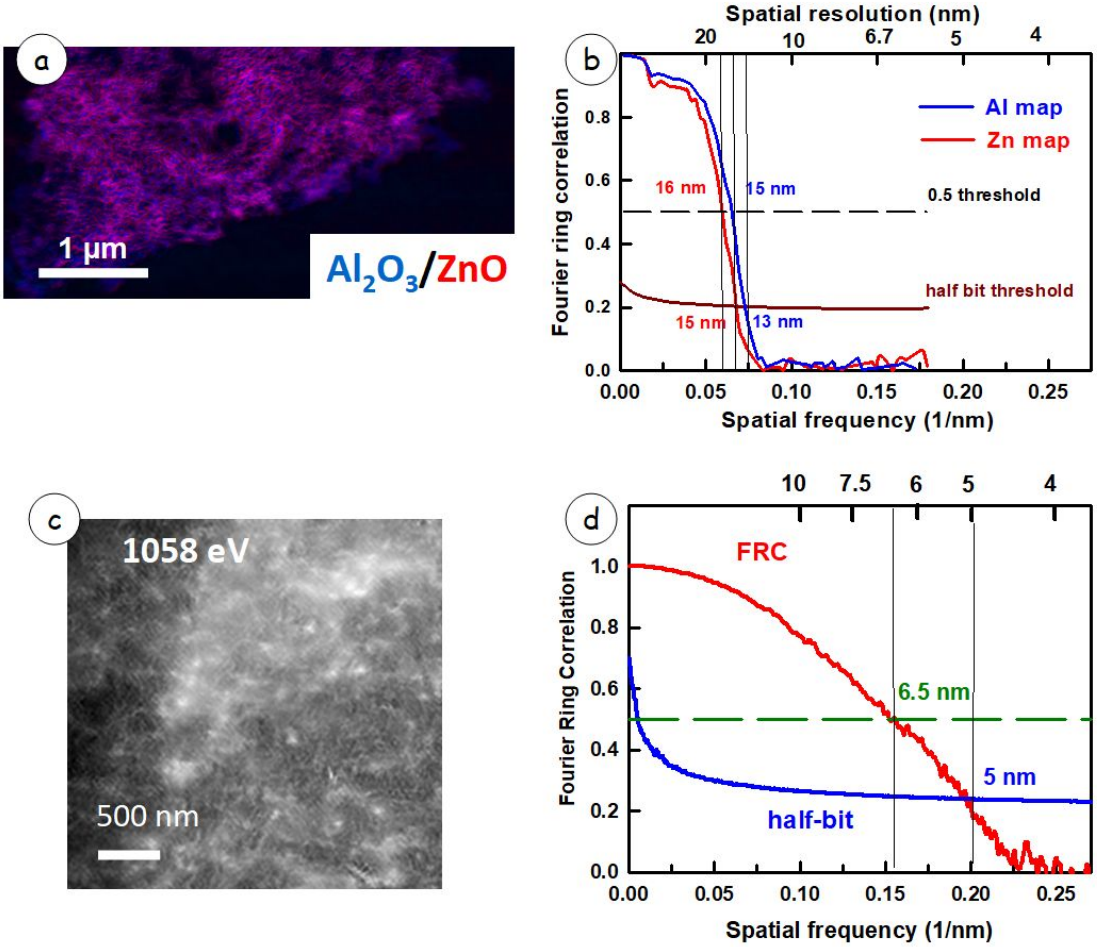

Figure S6 (a) Color coded composite of ZnO (red) and Al_2O_3 (blue) maps from ptychography of **sample A** (25-cycle) (b) Fourier Ring Correlation evaluations of the 2D spatial resolution of ptychography results shown in Fig. (SI-6a). (c) Single energy maps from ptychography image of **sample E** (6-cycle) recorded in the Zn L continuum at 1058 eV. (d) Fourier Ring Correlation evaluations of the 2D spatial resolution of ptychography results shown in Fig. (SI-6c).

SI-h Comparison of the impact on the 3D spatial resolution of the number of iterations of the compressed sensing (CS) tomography reconstruction

Figure S7 compares the spatial resolution, analyzed by Fourier shell correlation, of the same 3D Al_2O_3 framework volume, reconstructed by 50 and 200 iterations of the compressed sensing algorithm The resolution estimations with 1/2-bit (magenta solid line) threshold criteria are 8.85 nm for 50 iterations (red solid line with scatter) and 8.70 nm for 200 iterations (green solid line with scatter). A slight improvement in the 3D spatial resolution was observed by increasing the number of iterations of the CS tomographic reconstruction but this did not affect the main conclusions of the analysis.

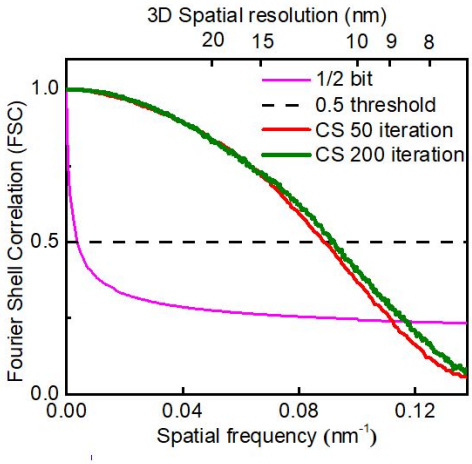

Figure S7 Spatial resolution from Fourier shell correlation of the 3D Al_2O_3 framework volumes of **Sample F** reconstructed by compressed sensing algorithm using 50 and 200 iterations.

SI-i Zn L-edge and Al K-edge spectroscopy of 6-cycle ZnO/Al_2O_3 before and after spectro-ptycho-tomography

In order to check for possible radiation damage by the very high flux of X-rays used in making the ptychography measurements we compare the Zn L and Al K spectra before and after spectro-ptycho-tomography on 6-cycle **sample F** (Xe FIB#2). The typical incident flux used in STXM imaging is 10^7 ph/s, whereas the typical incident flux used in ptychography measurements at the COSMIC beamline is ~10^9 ph/s. In addition, even 100 photon energy STXM spectra only have the beam on any single position on the sample for ~1 second total (STXM dwell times are typically 1-3 ms). In contrast a dwell time of 100 ms was typically used in measuring each sample point by ptychography. Given that ptychography was measured at 4 energies, at each of 15 angles, the overall dose was ~100 times larger in ptychography than in STXM. Despite this high dose, no significant changes were found when the Zn L and Al K-edge spectra measured before and after the ptychography measurements on **sample F** are compared **(see Figure S8)**.

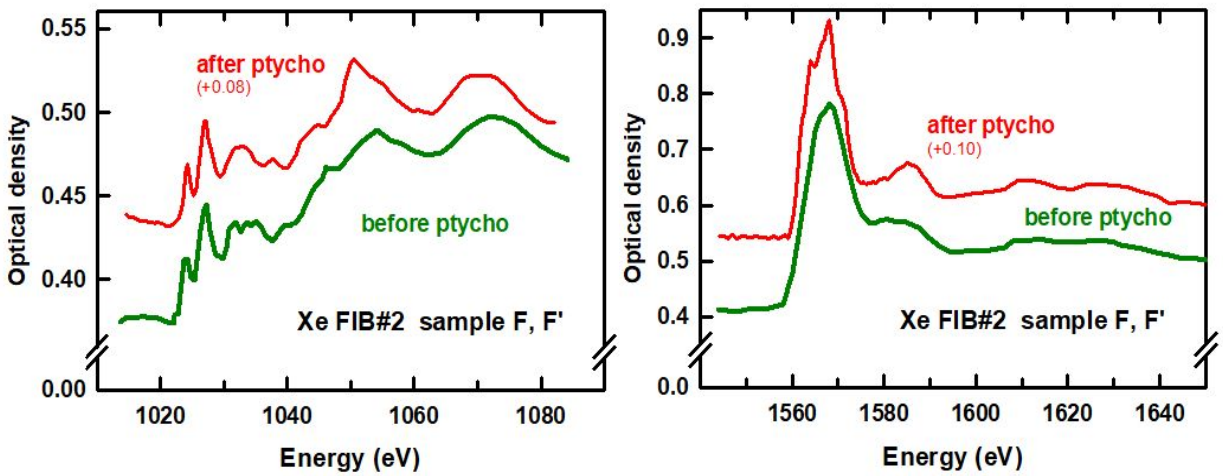

Figure S8 (a) Comparison of Zn L-edge spectra of **sample F** (Xe FIB#2, 6-cycle) before and after the spectro-ptycho-tomography measurements. (b) Comparison of Al K-edge spectra of **sample F** (Xe FIB#2, 6-cycle) before (F) and after (F') the spectro-ptycho-tomography measurements. In each plot, an offset of the post-ptycho spectrum has been used to show the spectra more clearly.

SI-j Relative concentration (RC) analysis of the 6-cycle, 12-cycle and 25-cycle samples

In order to quantitatively evaluate the spatial distributions of Al_2O_3, ZnO and porosity in the 3 different aerogels, the relative concentration (RC) [44] of each species was calculated as a function of distance across the central 1 μm^3 volume unit (in the direction along the long-axis of the FIB cylinder), with the results shown in **Fig. S9**. RC is defined as the ratio of the amount of one species relative to the sum of all species, averaged over a number of voxels. The results are shown for the 6-cycle (**Fig. S9a**), 12-cycle (**Fig. S9b**) and 25-cycle (**Fig. S9c**). A similar plot for a different volume of the 25-cycle sample was published earlier [7]. In **Fig. S9** the RC of "only Al_2O_3" is plotted in blue, "only ZnO" in red, "porosity" in black and colocalization (both Al_2O_3 and ZnO) in green as a function of the distance along the z-axis across the central 1 μm^3.

Fig. 6c and **Fig. S9** show that the Al_2O_3 aerogel scaffold retains its shape and thus concentration in the selected volume unit for both materials, which makes the comparison of ALD coating deposition cycles more convincing. The average of "only ZnO" RC increases from 16 to 19 vol % when the # of ALD deposition cycles increases from 6 to 12. This is accompanied by a decrease in the porosity fraction, as the ZnO partially fills the pore volume. However, if we compare the RC of the colocalized voxels (ones with both Al_2O_3 and ZnO) in the 6-cycle with that in the 12-cycle sample, the average value of the colocalized signal increases from 2 to 7 vol %. This indicates that the area of the Al_2O_3 framework coated by ZnO increases as the number of ALD deposition cycles increases. The distribution of both "only Al_2O_3" and "only ZnO" are relatively uniform in the 12-cycle sample (**Fig. S9b**), while the "only ZnO" in the 6-cycle sample (**Fig. S9a**) has a higher modulation along the z-axis in the selective volume. For both materials, the "only ZnO" distribution has a higher RC at positions where the Al_2O_3 framework has a lower concentration, while the colocalized layers show a similar trend with the evolution of Al_2O_3 scaffold. Since the 3D spatial resolution of the chemically-selective ptycho-tomography results for the 25 cycle ZnO/

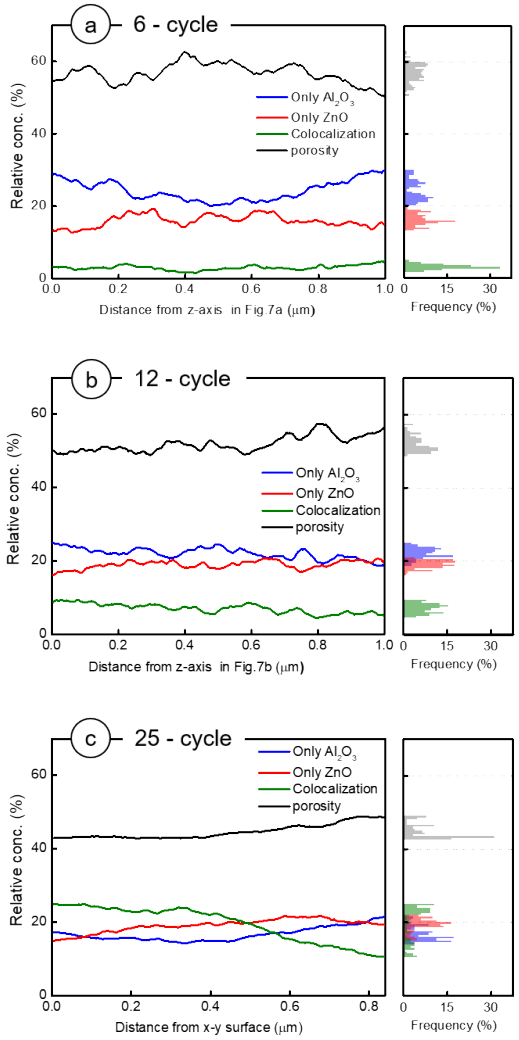

Figure S9. Relative concentration (RC) as a function of distance across the reconstructed volume of the two pure components (Al_2O_3 in blue and ZnO in red) along the *z*-axis (along the FIB cylinder) in the selected 1×1×1 μm^3 volume unit shown in Fig.7a and Fig. 7b, in the (a) 6-cycle sample (Xe-FIB#2, **sample F**), averaged in (*x*,*y*) over 192×192 voxels; and (b) 6 cycle sample (Xe-FIB#3, sample H), averaged in (*x*,*y*) over 208×208 voxels, Ostu threshold were applied the same as in Fig 7 (COSMIC, March & October, 2019); (c) 25-cycle sample (**sample A**), averaged in (x,y) over 83×83 voxels; Ostu threshold were applied [7]. The distribution of voxels that contain both Al_2O_3 and ZnO above the segmentation threshold (i.e. where Al_2O_3 and ZnO are colocalized) is plotted in green. The black curve indicates the fraction of porosity - the volume with neither material present. The plots at the right of the figure display the frequency distribution of RC values, using the same color coding.

Al_2O_3 aerogel (**sample A**) is much lower (~30 nm, versus 9 nm for the 6- and 12-cycle data) detailed comparisons of this type cannot be extended to the 25-cycle sample. Instead for the remainder of this section, we discuss the effect of the number of ALD cycles on material structural properties based on data from only the 6 and 12 cycle samples.

The spatial distribution of Al_2O_3, ZnO and colocalization in 2D slices extracted from the tomography reconstruction can provide an alternative visualization and a deeper understanding of the structure of these ZnO/ Al_2O_3 aerogels. **Fig. S10** shows color-coded composite maps of a 10 nm slice cut in the y*z* plane from the tomographic reconstruction results of 6- and - cycle ALD coated aerogels, respectively. These slices are extracted from the same 1 μm^3 volume shown in **Fig. 6**. The ZnO signal in the 6-cycle sample is in the form of discrete quasi-circular dots whereas the Al_2O_3 signal forms a continuous scaffold (**Fig. 5a**). However, the ZnO signal in the 12-cycle sample presents more elongated particles, more similar to the Al_2O_3 distribution. As the thickness of the extracted slice increases the ZnO distribution becomes more 'ribbon-like', but is still closely aligned with the Al_2O_3 framework (see **Fig. S10c**). A much higher fraction of colocalized signal is found in the 12-cycle sample, (pixels colored purple in **Fig. S10c**), consistent with the expectation that increasing the number of ALD cycles from 6 to 12 increases the surface coverage of ZnO on the Al_2O_3 substrate.

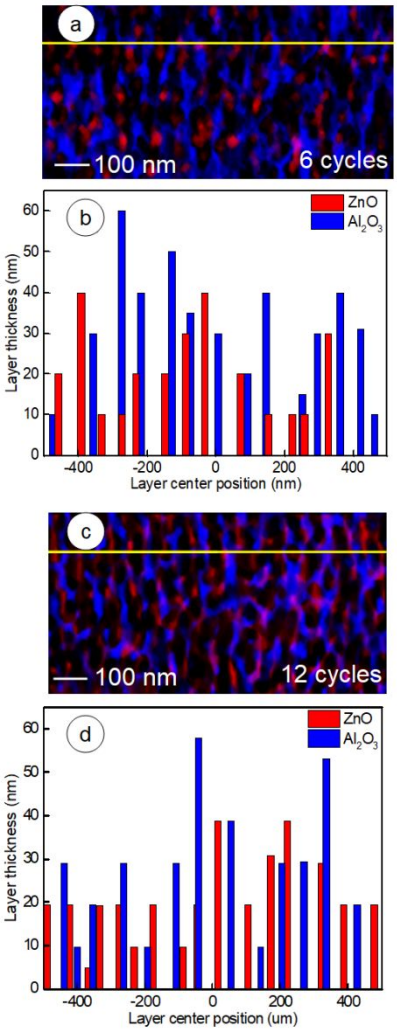

Figure S10. (a) Color coded map of a 10 nm slice extracted from the tomographic reconstruction of the 6-cycle sample (Xe-FIB#2, **sample F)** (b) The thickness profile of the ZnO (red) and Al_2O_3 (blue) along the yellow line in Fig. S10a. (c) Color coded map of a 10 nm slice extracted from the tomographic reconstruction of the 12 cycle aerogel sample (Xe-FIB#3, **sample H**). (d) the thickness profile of the ZnO (red) and Al_2O_3 (blue) along the yellow line in Fig. S10c.

The histograms in **Fig. S10b** and **Fig. S10d** show the position and thickness of the ZnO and Al_2O_3 layers along the z-axis, perpendicular to the yellow line indicated in the plane of the slice. 13 layers of Al_2O_3 scaffold were encountered along the 1 μm path in the 6-cycle sample (**Fig. S10b**), while 12 layers of Al_2O_3 scaffold were encountered along the 1 μm path in the 12-cycle sample. The distributions of the thickness of Al_2O_3 are similar in both samples, from 10 to 60 nm. However, for the ZnO distribution, there were 12 particles encountered in the 6-cycle sample, and 16 ZnO particles encountered in the 12-cycle sample. A few Al_2O_3 layers in the 12-cycle sample have ZnO coating attached on both sides. In addition, unlike the more uniform thickness distribution of the ZnO coating in the 12-cycle sample, there is a higher scatter in the thickness distribution of ZnO in the 6-cycle material (compare **Figs. S10b** and **S10d**).

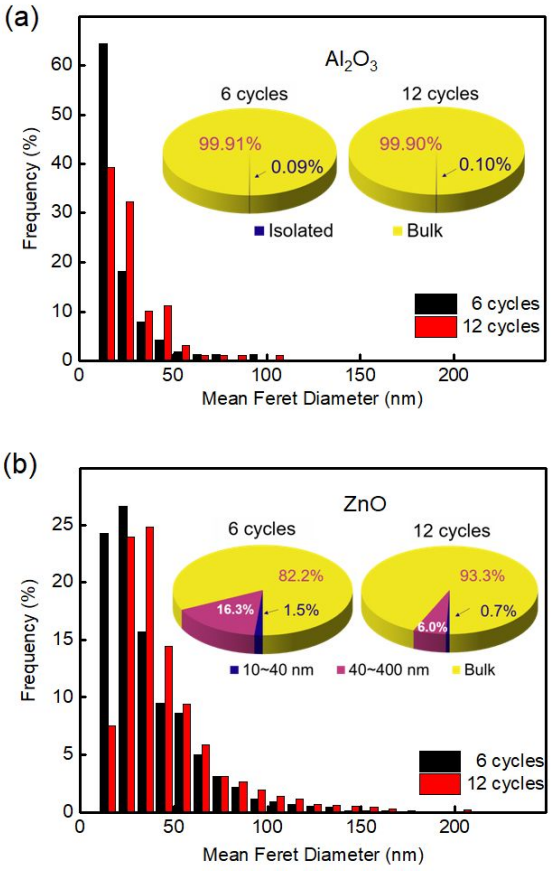

Figure S11 (a) Distribution of the Feret diameter (bar plot) of isolated individual Al_2O_3 entities in the aerogel material, and their fraction of the entire Al_2O_3 volume for 6-cycle (Xe-FIB#2, **sample F,** black) and 12-cycle (Xe-FIB#3, **sample H**, red) ALD coated aerogels in a selected 2×2×2 μm^3 volume of sample; (b) Distribution of Feret diameter (bar plot) of isolated individual ZnO crystals in the materials, and their fraction of the entire ZnO volume in a selected 2×2×2 μm^3 volume of sample.

SI-j Effect of changing the volume analysed on size distributions

Figure S11 shows the distribution of the isolated Al_2O_3 and ZnO particles inside the central 2×2×2 μm^3 volume of the 6-cycle and 12-cycle samples, analysed using the mean Feret diameter. **Figure S11a** shows the frequency distribution histogram of Feret diameter of the segmented Al_2O_3 crystal/layer in the 6 and 12 cycles materials. The results of analysis of the 2×2×2 μm^3 volume are very similar to those from the size distribution analysis of the 1×1×1 μm^3 volume as shown in **Fig. 7** (main paper), with only a slight

increase of the bulk ZnO (~0.2%) and bulk Al_2O_3 (~0.05%) fraction. If the analysis was biased by artefacts in the ~50 nm adjacent to the edge of the analysed volume, such artefacts would be decreased by a factor of 8 when going from the $(1\ \mu m)^3$ to the $(2\ \mu m)^3$ volume.

SI-k Distributions of the specific surface area (SSA) of individual ZnO crystals

Figure S12 shows the distributions of the specific surface area (SSA) of the individual ZnO crystals segmented from the $1\times1\times1\ \mu m^3$ chunked volume of the 6-cycle (**sample F)** and 12-cycle (**sample H**) samples, respectively. The ZnO crystal sizes are classified into 2 groups: i) Feret diameters range 10~40 nm ($>0.28 nm^{-1}$), and ii) Feret diameters >40 nm ($0.13\sim0.28\ nm^{-1}$). The 12-cycle ALD coating sample has a smaller SSA distribution than that of 6-cycle sample.

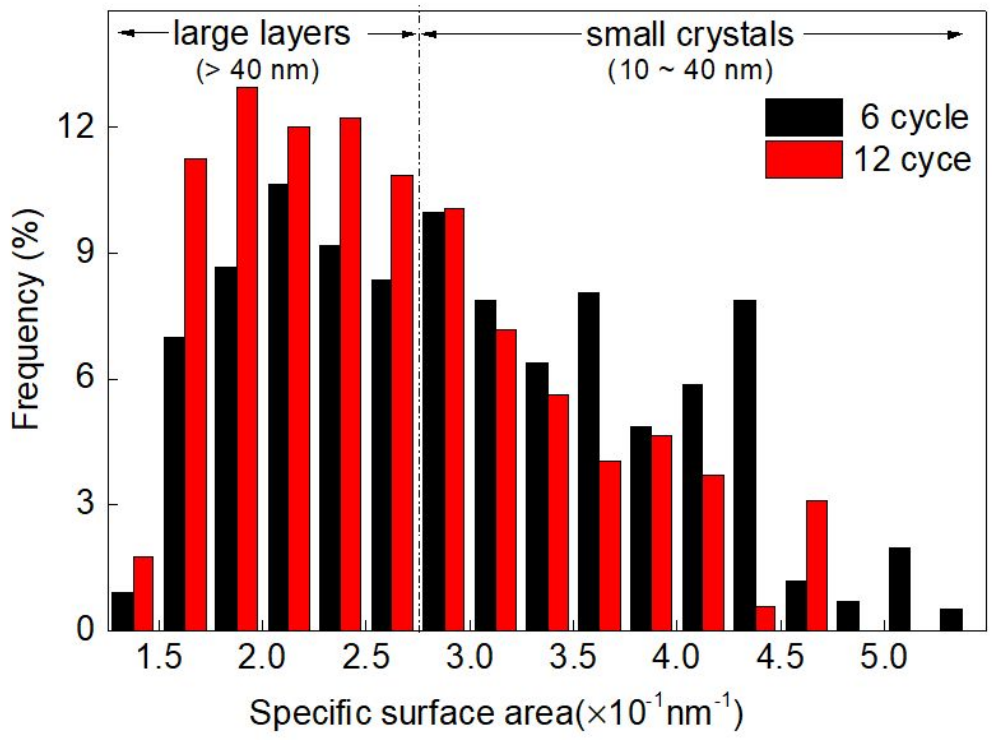

Figure S12 Distributions of the specific surface area (SSA) of the individual ZnO crystals segmented from the $(1\times1\times1)\ \mu m^3$ volume extracted from the centre of the ZnO tomograms of the 6-cycle (**sample F)** and 12-cycle (**sample H**) samples.

SI-l Volume fraction, surface area and SSA of Al_2O_3 and ZnO inside the central (2×2×2) µm^3 volume

Table S3. Volume fraction, surface area and specific surface area (SSA) of Al_2O_3 and ZnO components inside a selected 2×2×2 µm^3 volume of the 6 and 12 cycle ZnO/Al_2O_3 aerogel samples.

Sample →	6 cycles ALD [(a)]		12 cycles ALD [(b)]	
Component →	Al_2O_3	ZnO	Al_2O_3	ZnO
Volume (×10^8 nm^3)	20.3 ± 0.3	14.3 ± 0.3	20.7 ± 0.3	17.6 ± 0.2
Surface Area (×10^7 nm^2)	27.0 ± 0.5	22.5 ± 0.2	28.4 ± 0.4	23.5 ± 0.2
SSA (×10^{-1} nm^{-1})	1.3 ± 0.1	1.6 ± 0.1	1.4 ± 0.1	1.3 ± 0.1

(a) Otsu thresholds used for segmenting the 6 cycle ALD sample F: 7.3x10^{-4} (Al_2O_3) and 6.3x10^{-4} (ZnO).

(b) Otsu thresholds used for segmenting the 12 cycle ALD sample H: 4.7×10^{-4} (Al_2O_3) and 5.4×10^{-4} (ZnO).

SI-m Details of the movies of renderings of the 3D reconstruction of the spectro-ptycho-tomography results for the 6 cycle, sample F (Xe plasma FIB #2) and 12 cycle, sample H (Xe plasma FIB#3).

Movie S1: FIB volume cut-through movie

Filename: **movie-S1_ZnO-Al2O3-F-XeFIB2- cut_through.mp4**
Sample: **Sample F** (Xe plasma FIB #2)
Presented volume: 3.5×3.5×4 um^3
Threshold: $7.3x10^{-4}$ (OD/voxel) for Al_2O_3 and $6.3x10^{-4}$ for ZnO.
Rendering Mode: Volume rendering
Software: Dragonfly

Movie S2: Cut-out volume fly-through movie

Filename: **movie-S2_ZnO-Al2O3-H-XeFIB3- fly_through.mp4**
Sample: **Sample H** (Xe plasma FIB #3)
Presented volume: 1×1×1 um^3
Threshold: 4.72×10^{-4} (OD/voxel) for Al_2O_3 and 5.41×10^{-4} for ZnO.
Rendering Mode: Surface rendering
Software: Avizo

Movie S3: Pore connectivity movie

Filename: **movie-S3_ZnO-Al2O3-H-XeFIB3_pores.mp4**
Sample: **Sample H** (Xe plasma FIB #3)
Presented volume: 1×1×1 um^3
Threshold: ALL – (4.72×10^{-4} (OD/voxel) for Al_2O_3 and 5.41×10^{-4} for ZnO).
Rendering Mode: Volume rendering
Software: Avizo